Oncogene (2007) 26, 543–553

www.nature.com/onc

ORIGINAL ARTICLE

Loss of mammary epithelial prolactin receptor delays tumor formation by reducing cell proliferation in low-grade preinvasive lesions

SR Oakes[1], FG Robertson[1], JG Kench[2], M Gardiner-Garden[1], MP Wand[3], JE Green[4] and CJ Ormandy[1]

[1]*Cancer Research Program, Garvan Institute of Medical Research, Darlinghurst, Sydney, NSW, Australia;* [2]*Department of Tissue Pathology, Institute of Clinical Pathology and Medical Research, Westmead, NSW, Australia;* [3]*Department of Statistics, School of Mathematics, The University of New South Wales, Sydney, NSW, Australia and* [4]*Transgenic Oncogenesis Group, Laboratory of Cell Regulation and Carcinogenesis, Bethesda, Maryland, MD, USA*

Top quartile serum prolactin levels confer a twofold increase in the relative risk of developing breast cancer. Prolactin exerts this effect at an ill defined point in the carcinogenic process, via mechanisms involving direct action via prolactin receptors within mammary epithelium and/or indirect action through regulation of other hormones such as estrogen and progesterone. We have addressed these questions by examining mammary carcinogenesis in transplants of mouse mammary epithelium expressing the SV40T oncogene, with or without the prolactin receptor, using host animals with a normal endocrine system. In prolactin receptor knockout transplants the area of neoplasia was significantly smaller (7 versus 17%; $P<0.001$ at 22 weeks and 7 versus 14%; $P=0.009$ at 32 weeks). Low-grade neoplastic lesions displayed reduced BrdU incorporation rate (11.3 versus 17% $P=0.003$) but no change in apoptosis rate. Tumor latency increased (289 days versus 236 days, $P<0.001$). Tumor frequency, growth rate, morphology, cell proliferation and apoptosis were not altered. Thus, prolactin acts directly on the mammary epithelial cells to increase cell proliferation in preinvasive lesions, resulting in more neoplasia and acceleration of the transition to invasive carcinoma. Targeting of mammary prolactin signaling thus provides a strategy to prevent the early progression of neoplasia to invasive carcinoma.

Oncogene (2007) **26,** 543–553. doi:10.1038/sj.onc.1209838; published online 24 July 2006

Keywords: prolactin receptor; mouse; mammary; carcinogenesis; C3(1)/SV40T

Correspondence: Professor CJ Ormandy, Garvan Institute of Medical Research, St Vincent's Hospital, 384 Victoria St, Darlinghurst, Sydney, NSW 2010, Australia.
E-mail: c.ormandy@garvan.org.au
Financial Support: US CDMRP Predoctoral Scholarship DAMD 17-03-1-0686, National Health and Medical Research Council.
Received 22 March 2006; revised 8 June 2006; accepted 22 June 2006; published online 24 July 2006

Introduction

The Nurses Health Study I (http://www.channing.harvard.edu/nhs/) is a large prospective study begun in 1976. A case–control study conducted using this cohort examined the risk of breast cancer conferred by elevated serum prolactin levels. Blood samples were collected between 1989 and 1990, and 306 postmenopausal women were subsequently diagnosed with breast cancer before 1994. These women were matched to 448 control subjects. Measurement of serum prolactin demonstrated that top quartile serum prolactin (PRL) conferred a higher relative risk (2.03-fold 95%CI 1.24–3.31 $P=0.01$) of developing breast cancer compared to women with bottom quartile serum prolactin (Hankinson *et al*., 1999). The effect was independent of plasma sex steroid hormones and exclusion of cases diagnosed within 2 years of blood collection resulted in the same conclusion. The cohort was updated with 851 cases diagnosed by 2000, matched to 1275 controls (Tworoger *et al*., 2004). Overall the same positive correlation between breast cancer risk and serum prolactin levels was seen (1.35-fold 95%CI 1.02–1.76 $P=0.01$), and this association varied by sex hormone receptor status, with ER+ PR+ tumors having an increased relative risk of 1.78 (95% CI, 1.28, 2.50; P-trend <0.001) compared to ER− tumors (0.76 95% CI, 0.43, 1.32; P-trend $=0.28$).

Rodent cancer models recapitulate the sensitivity of the human breast to PRL (Welsch and Nagasawa, 1977; Wennbo and Tornell, 2000). Pituitary grafts or transgenic strategies that increase serum Prl levels result in mammary cancer. For example, transgenic mice that overexpress human growth hormone, which binds both Prlr and growth hormone receptors, develop mammary carcinoma while mice over expressing the growth hormone receptor-restricted ligand bGH do not (Wennbo *et al*., 1997). Overexpression of rat Prl using the lipocalin promoter to drive expression predominantly in mammary epithelium produces (ER) positive tumors at a higher rate than other mouse mammary cancer models (Rose-Hellekant *et al*., 2003). Prl as a modulator of preinitiated cancer has been examined in chemical carcinogenesis (Welsch *et al*., 1975) and transgenic oncogene models. Prl and Prlr mRNA were

detected in nitrosomethylurea (NMU) carcinogen-induced tumors and a rat Prl antiserum inhibited NMU-induced tumor cell proliferation by up to 70%, compared to normal rabbit serum and GH antiserum (Mershon *et al*., 1995). Mice expressing the polyoma middle-T antigen oncogene develop tumors in the first weeks of life, but when crossed with Prl knockout mice they developed tumors significantly later (Vomachka *et al*., 2000). These, and other experiments, have demonstrated that Prl alone at high levels is sufficient to produce mammary cancer, and that its loss can retard tumor formation in response to an oncogenic stimulus.

The mechanisms behind these important observations are not clear. It has generally been assumed that prolactin exerts its effects via direct modulation of the mammary epithelial cell (reviewed Vonderhaar, 1999; Clevenger *et al*., 2003) and there is evidence consistent with this. Thus, prolactin receptors (PRLR) are expressed at high levels predominantly by steroid hormone receptor positive breast cancer cells and tumors (Bonneterre *et al*., 1987; Ormandy *et al*., 1997c), but at low levels by most tumors (Reynolds *et al*., 1997). Prolactin causes an increase in proliferation (Ginsburg and Vonderhaar, 1995; Das and Vonderhaar, 1997; Llovera *et al*., 2000) and cyclin D1 expression (Schroeder *et al*., 2003) in breast cancer cell lines selected for prolactin sensitivity (Schroeder *et al*., 2002). Likewise the use of PRLR antagonists can reduce proliferation (Goffin *et al*., 1996; Chen *et al*., 1999; Llovera *et al*., 2000) in some breast cancer cell lines. PRL is also produced by mammary epithelial cells and has been hypothesized to act via an autocrine mechanism (Clevenger *et al*., 1995; Ginsburg and Vonderhaar, 1995; Reynolds *et al*., 1997). Transplants of mouse mammary epithelium lacking the Prl gene show normal development during pregnancy, but show a threefold reduction in cell proliferation at parturition, the time at which PRL production by the epithelium becomes apparent (Naylor *et al*., 2003). PRL may also exert a direct effect via the modulation of the sensitivity of the epithelial cell to the action of other hormones. For example, exogenous Prl modulates the expression of progesterone receptors by human breast cancer cells (Ormandy *et al*., 1997c), while endogenous PRL can influence estrogen receptor (ER) alpha levels (Gutzman *et al*., 2004).

Recent work in mice, however, demonstrates that prolactin also exerts potent indirect effects on the mammary gland via modulation of the systemic endocrine system. Null mutation of Prl or Prlr in mice (Horseman *et al*., 1997; Ormandy *et al*., 1997a) results in disruption of ovarian, pituitary and other endocrine systems (Clement-Lacroix *et al*., 1999). Thus, failed mammary ductal side branching during ductal morphogenesis is restored by transplanting $Prlr^{-/-}$ epithelium into the cleared fat pads of hosts with normal endocrine function (Brisken *et al*., 1999) or by progesterone pellet administration (Binart *et al*., 2000). Modulation of the endocrine system by prolactin provides a potential mechanism underlying the results to date in mouse models and the Nurses Health Study.

We have scant knowledge regarding the point in the carcinogenic process where prolactin exerts its effect. It may exert an effect as a continuation of its normal developmental role, or acquire a novel role due to dysregulation in cancer. There is evidence for the latter. Prlr expression is increased in cancer compared to adjacent normal tissue (Touraine *et al*., 1998). Alternatively altered ratios of a number of different splicing variants and isoforms could modulate signaling from this receptor in cancer (Clevenger *et al*., 1995). The C3(1)SV40T model of mammary cancer provides a reproducible series of defined neoplastic lesions that progress to invasive carcinoma and resemble the human disease (Maroulakou *et al*., 1994; Shibata *et al*., 1998; Green *et al*., 2000). In combination with genetic deletion of the Prlr, this provides an ideal model to investigate where in the carcinogenic process prolactin acts. By using mammary epithelial transplantation to remove the disruption to the ovarian–pituitary endocrine axis that is caused by systemic deletion of the Prlr, we can distinguish the direct and indirect actions of Prl. We have used this approach to examine the questions of direct or indirect action and point of influence in the carcinogenic process.

Results

Tumor formation in $Prlr^{-/-}$/C3(1)/SV40T and WT/C3(1)/SV40T mice

The development of palpable tumors was monitored in $Prlr^{-/-}$ and WT mice that carried the C3(1)/SV40T construct. C3(1)/SV40T mice which lacked Prlr had significantly increased latency to palpable tumor formation (200 ± 9 days) compared to control C3(1)/SV40T mice (175 ± 7 days, logrank $P = 0.033$; Figure 1a). $Prlr^{-/-}$/C3(1)/SV40T mice also reached a tumor burden of 10% body weight significantly later (243 ± 15 days) compared to WT/C3(1)/SV40T mice (217 ± 15 days, logrank $P = 0.032$; Figure 1b). To determine whether Prlr signaling affected tumor growth rate, a mixed effects linear model was applied to the cubed root of tumor volume for each experimental animal group. Tumors that were filled with fluid at the ethical end point were excluded from the analysis. Results are plotted with day 0 as the day the tumor was detected (Figure 1c). No significant difference in the rate of change in tumor volume was detected in $Prlr^{-/-}$/C3(1)/SV40T mice compared to control C3(1)/SV40T mice ($P = 0.45$).

Tumor morphology in $Prlr^{-/-}$/C3(1)/SV40T and WT/C3(1)/SV40T mice

Histological examination of tumor tissues collected at the ethical end point was undertaken (Table 1). Some of the smaller tumors exhibited areas that had not yet invaded through the basement membrane and represent a stage similar to human ductal carcinoma *in situ*. The invasive tumors demonstrated a high-grade morphology, high mitotic index, coarse chromatin structure, pleomorphic nuclei and foci of necrosis. Tumors often

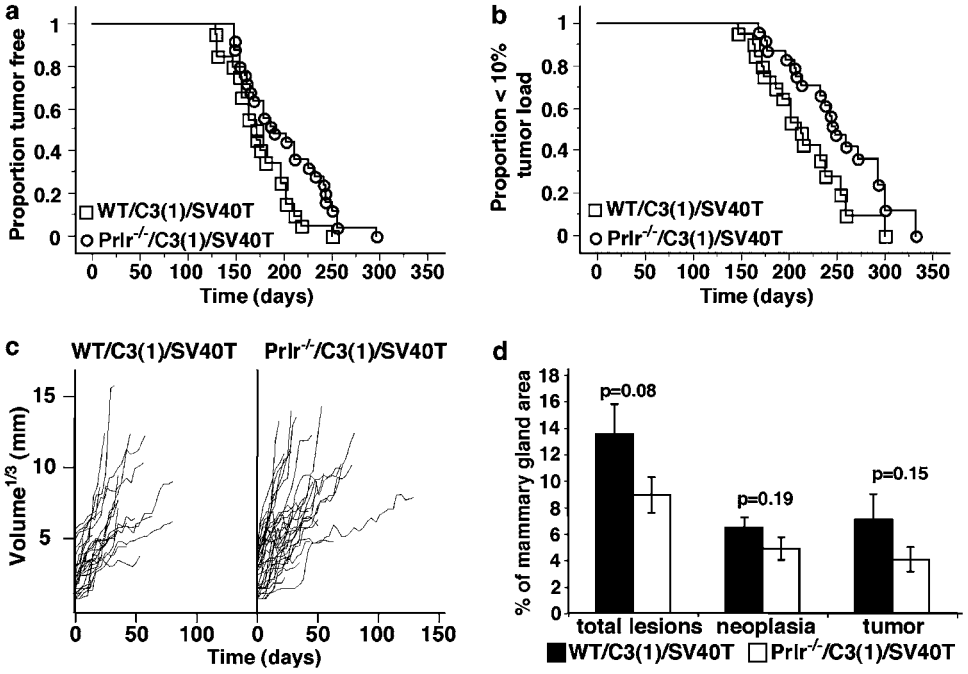

Figure 1 Tumor formation in Prlr$^{-/-}$/C3(1)/SV40T mice (**a**) Tumor-free survival curve (Kaplan–Meier). Time is represented in days after birth. Prlr$^{-/-}$/C3(1)/SV40T mice (circles) develop palpable tumors significantly later compared to WT/C3(1)/SV40T mice (squares, $P=0.033$). (**b**) Survival curve. Time is represented in days after birth. Prlr$^{-/-}$/C3(1)/SV40T mice (circles) reach the ethical end point of 10% tumor burden significantly later than WT/C3(1)/SV40T mice (squares, $P=0.032$). (**c**) Tumor volume trellis plot. The cube root of tumor volume (volume$^{1/3}$) is plotted with respect to time after detection (days). Time 0 is the day of initial detection. There was no significant difference in the rate of change in tumor volume from WT/C3(1)/SV40T mice (left box) and Prlr$^{-/-}$/C3(1)/SV40T mice (right box) ($P=0.45$). (**d**) Bar graph summary of mammary whole-mount analysis. Prlr$^{-/-}$/C3(1)/SV40T mice (white bars) showed a trend towards reduced area of lesions as a percentage of total mammary fat pad area compared to WT/C3(1)/SV40T mice (black bars, $P=0.08$). The area of lesions when classified into neoplasia and tumor was reduced in Prlr$^{-/-}$/C3(1)/SV40T mice compared to WT/C3(1)/SV40T mice although this was not statistically significant ($P=0.19$ and $P=0.15$, respectively).

Table 1 Tumor morphology and cellular structure in tumors from WT/C3(1)/SV40T and Prlr$^{-/-}$/C3(1)/SV40T mice

		% Area of tumor			*Cellular structure*	
Epithelium genotype	n	*Acinar/Glandular*	*Papillary*	*Solid*	*Type A*	*Type B*
Reached 10% tumor burden						
WT/C3(1)/SV40T	30	17±3	11±3	72±5	67	33
Prlr$^{-/-}$/C3(1)/SV40T	29	18±3	19±5	63±6	74	26
P-value		0.86	0.19	0.25	χ^2 $P=0.28$	
Did not reach 10% tumor burden						
WT/C3(1)/SV40T	12	23±4	16±7	61±8	77	23
Prlr$^{-/-}$/C3(1)/SV40T	20	15±3	10±4	75±6	67	33
P-value		0.14	0.46	0.17	χ^2 $P=0.12$	
All tumors collected						
WT/C3(1)/SV40T	42	19±3	12±3	69±4	70	30
Prlr$^{-/-}$/C3(1)/SV40T	49	17±2	15±4	68±4	71	29
P-value		0.49	0.47	0.84	χ^2 $P=0.88$	

n; number of tumors. The average percent of tumor area classified as acinar and/or glandular, papillary and solid is given±s.e. The percentage of tumors classified as having type A or type B cellular structure is also shown.

displayed more than one low-power architectural pattern including acinar and/or glandular, papillary and solid areas. Acinar and glandular patterns were grouped together for analysis as they often tended to merge into each other rendering reliable distinction problematic. These pathologies have been described in detail previously (Cardiff *et al*., 2000). Cellular morphology demonstrated two main variants: firstly tumor cells with a high nucleocytoplasmic ratio, hyperchromatic nuclei, coarse chromatin and mild to moderate pleomorphism designated (Type A); and secondly cells with a lower nucleocytoplasmic ratio, a smaller amount

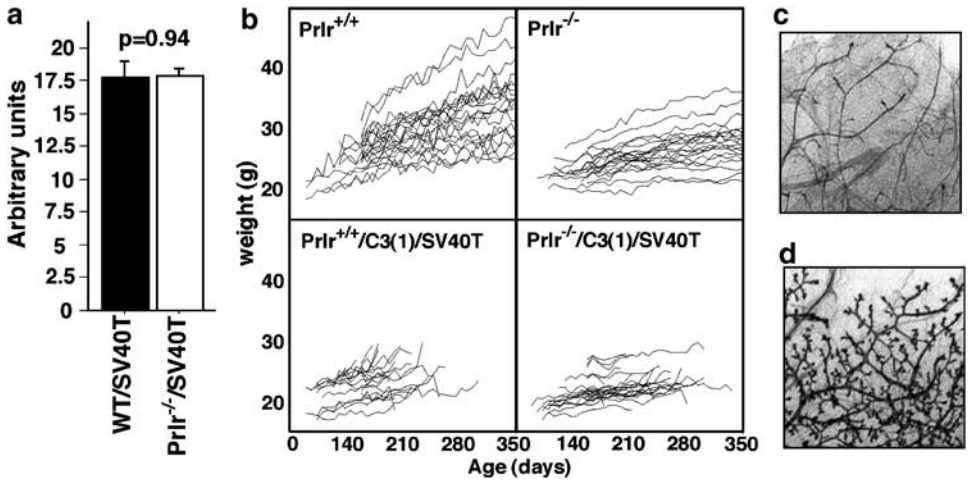

Figure 2 SV40T expression, body weight and mammary morphology in Prlr$^{-/-}$/C3(1)/SV40T mice (**a**) Bar graph of relative SV40T mRNA expression. There was no significant difference in the relative expression of SV40T mRNA in the inguinal mammary glands from WT/C3(1)/SV40T mice and Prlr$^{-/-}$/C3(1)/SV40T ($P=0.94$) (**b**) Body weight trellis plot for WT (top left) and Prlr$^{-/-}$ (top right) mice and WT/C3(1)/SV40T (bottom left) and Prlr$^{-/-}$/C3(1)/SV40T (bottom right) transplants. Age (days) is represented on the horizontal axis and body weight (grams) on the vertical axis. The increase in body weight is significantly more gradual in Prlr$^{-/-}$ and Prlr$^{-/-}$/C3(1)/SV40T compared to control WT and WT/C3(1)/SV40T ($P=0.006$ and $P=0.005$, respectively). (**c**) Prlr$^{-/-}$/C3(1)/SV40T inguinal mammary gland, Carmine stain. (**d**) WT/C3(1)/SV40T inguinal mammary gland, Carmine stain.

of eosinophilic cytoplasm, more vesicular chromatin and more marked pleomorphism (Type B). Some tumors demonstrated intermediate forms and were classified according to the predominant features. Areas of necrosis were observed in 98% of tumors at collection. Statistical analysis of tumor classification in a blinded fashion revealed no significant difference in tumor architecture or cellular morphology between tumors derived from Prlr$^{-/-}$/C3(1)/SV40T mice or control C3(1)/SV40T mice.

Mammary neoplasia in Prlr$^{-/-}$/C3(1)/SV40T and WT/C3(1)/SV40T mice

Mammary whole mounts were analysed for the development of neoplastic lesions. Analysis of mammary whole mounts collected at the ethical end point (Figure 1d) demonstrated that C3(1)/SV40T mice that lacked Prlr displayed a trend toward reduced lesion-area measured as a percentage of total mammary fat pad area ($8.9\pm1.3\%$) compared to WT/C3(1)/SV40T mice at the ethical end point ($13.6\pm2.2\%$, $P=0.08$).

SV40T levels in Prlr$^{-/-}$/C3(1)/SV40T and WT/C3(1)/SV40T mice

Some mammary specific promotors such as MMTV and WAP are sensitive to pregnancy and/or hormone stimuli (Hutchinson and Muller, 2000). This complicates investigation of endocrine-mediated carcinogenesis as observed effects may simply be due to changes in transgene expression. The C3(1) rat prostatic steroid-binding protein (PSBP) promoter used here is not steroid hormone responsive (Shibata *et al*., 1998; Green *et al*., 2000). To confirm that SV40T expression was not altered by Prlr genotype, quantitative real time PCR was used to examine the relative expression of SV40T mRNA. Expression of SV40T mRNA was detected in all mammary glands from 12 week C3(1)/SV40T inguinal mammary glands (Figure 2a). There was no significant difference in the relative expression of SV40T between mammary glands from 12-week-old WT/C3(1)/SV40T (18 ± 0.5 U) and Prlr$^{-/-}$/C3(1)/SV40T mice (18 ± 1.2 U, *t*-test $P=0.94$).

Body weight and mammary gland morphology in Prlr$^{-/-}$/C3(1)/SV40T and WT/C3(1)/SV40T mice

To determine if Prlr$^{-/-}$ mice differ in body weight compared to control mice, both WT and C3(1)/SV40T animals were aged and weighed weekly. A mixed effects linear model demonstrated that both Prlr$^{-/-}$ and Prlr$^{-/-}$/C3(1)/SV40T animals gained weight at a reduced rate compared to WT and WT/C3(1)/SV40T mice ($P=0.006$ and $P=0.005$, respectively; Figure 2b). Control Prlr$^{-/-}$ mice were approximately 17% lighter (average 27.8 ± 0.8 g) at 50 weeks of age compared to control WT mice (average 33.6 ± 1.3 g). Reduced body weight in female Prlr$^{-/-}$ mice is due to reduced abdominal fat stores via a mechanism that includes altered endocrine environment (Freemark *et al*., 2001) and possibly Prlr expression by adipocytes (Ling *et al*., 2000). Mammary whole mounts (Figure 2c) collected from these mice at 50 weeks demonstrated a failure of ductal side branching in Prlr$^{-/-}$ animals compared to WT (Figure 2d), as reported previously in prolactin and prolactin receptor knockout (Horseman *et al*., 1997; Ormandy *et al*., 1997a). These results are due to Prl modulation of progesterone levels via the pituitary–ovarian axis (Binart *et al*., 2000). These changes in body weight and mammary epithelial cell content potentially confound our results regarding altered tumor latency. These problems also potentially confound the results

obtained in many other rodent models of Prl action. Increased Prl levels produced via pituitary graft, Prl injection or transgenic methods, or loss of Prl produced by knockout or pituitary ablation, may have altered the systemic hormonal environment causing undetected changes in body weight and mammary epithelial cell number. To investigate this problem, we utilized mammary epithelial transplantation. This procedure rescues the defect in ductal side branching and negates the body weight issue by placing the test glands in a normal endocrine environment (Brisken *et al*., 1999).

Tumor formation in Prlr$^{-/-}$/C3(1)/SV40T and WT/C3(1)/SV40T transplants

Mammary glands made from Prlr$^{-/-}$ epithelium developed palpable tumors significantly later than mammary glands with WT/C3(1)/SV40T epithelium (289$\pm$22 days verses 236$\pm$24 days, logrank $P<0.001$; Figure 3a). We looked directly for an effect of Prlr genotype on tumor growth rate using a mixed effects linear model described above (Figure 3b). Tumors that were filled with fluid at ethical end point were excluded from the analysis. Overall there was no significant difference in the rate of tumor growth in tumors derived from Prlr$^{-/-}$/C3(1)/SV40T epithelium compared to tumors from WT/C3(1)/SV40T epithelium ($P=0.33$). WT/C3(1)/SV40T transplants produced a total of 29 tumors while Prlr$^{-/-}$/C3(1)/SV40T transplants produced 27, with mean tumors per transplant of 1.6$\pm$0.2 and 1.2$\pm$0.3, respectively, revealing no detectable significant ($P=0.23$) difference in tumor frequency between genotypes.

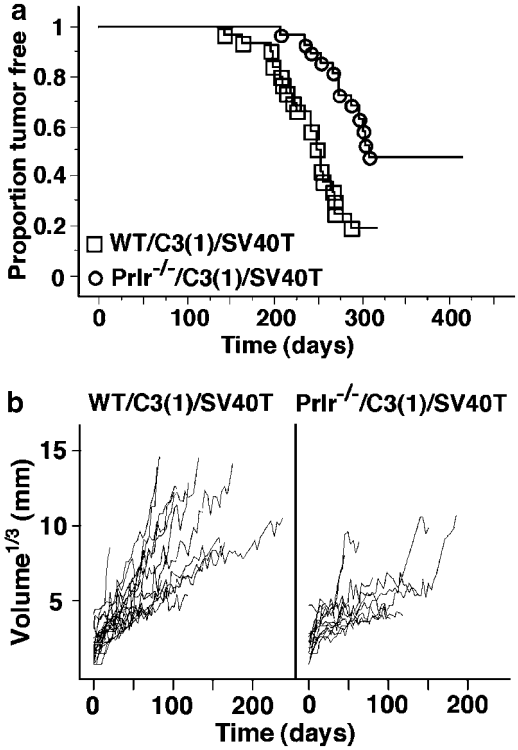

Figure 3 Tumor formation in Prlr$^{-/-}$/C3(1)/SV40T transplants (**a**) Tumor-free survival curve. Time is represented in days after transplantation. Palpable tumors were detected in Prlr$^{-/-}$/C3(1)/SV40T transplants (circles) significantly later compared to WT/C3(1)/SV40T transplants ($P<0.001$). (**b**) Tumor volume trellis plot. The cube root of tumor volume (volume$^{1/3}$) is plotted with respect to time (days). Time 0 is the day of initial detection. There was no significant difference in the rate of change in tumor volume from WT/C3(1)/SV40T transplants (left box) and Prlr$^{-/-}$/C3(1)/SV40T transplants (right box) ($P=0.33$).

SV40T expression is unaltered by loss of Prlr$^{-/-}$

We examined SV40T levels in 8 (56 days), 22 (154 days) and 32 week (224 days) old C3(1)/SV40T mammary glands formed by transplantation (Figure 4a). No significant difference was observed at 8, 22 and 32 weeks post surgery between WT/C3(1)/SV40T (16$\pm$0.8, 18$\pm$1.0 and 19$\pm$0.2 U) and Prlr$^{-/-}$/C3(1)/SV40T epithelial transplants (17$\pm$0.5, 18$\pm$0.3 and 19$\pm$0.3 U, $P=0.10$, $P=0.64$, $P=0.78$, respectively). Western blotting using an antibody against SV40T protein was used to determine the protein expression of SV40T in 8 week (56 day) old transplants (Figure 4b). Detection of

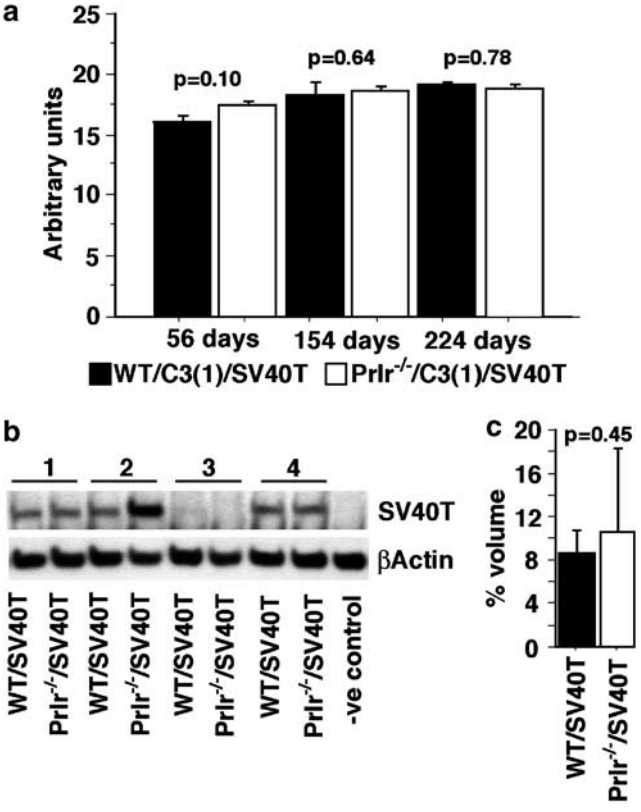

Figure 4 SV40T expression in Prlr$^{-/-}$/C3(1)/SV40T transplants (**a**) Relative expression of SV40T mRNA in 55 day (8 week), 154 (22 week) and 224 (32 week) old transplants. There was no significant difference in the expression of SV40T at 8, 22 and 32 weeks between Prlr$^{-/-}$/C3(1)/SV40T (white bars) and WT/C3(1)/SV40T (black bars) transplants ($P=0.10$, $P=0.64$, $P=0.78$, respectively). (**b**) Western blot of SV40T protein expression in 55 day (8 week) old transplants. β-actin is shown as a loading control. Four donor animals are indicated by the numbers above the blot. (**c**) Average volume of SV40T protein normalised to β-actin. There was no significant difference in the expression of SV40T protein between WT/C3(1)/SV40T (black bar) and Prlr$^{-/-}$/C3(1)/SV40T (white bar) 8 week old transplants.

β-actin protein was used as a loading control. The average volume of SV40T protein in WT/C3(1)/SV40T transplants was $8.6 \pm 0.7\%$ which was not significantly different to Prlr$^{-/-}$/C3(1)/SV40T transplants ($10.6 \pm 2.4\%$, $P = 0.45$), indicating that like the mRNA expression of SV40T, the protein expression of the transgene is not altered by the presence of the Prlr. Univariate regression analysis demonstrated that SV40T mRNA expression was not a predictor for age of detection ($P = 0.52$), tumor latency ($P = 0.95$) and days with tumor ($P = 0.52$).

Loss of Prlr within epithelium does not change the histology and morphology of SV40T-induced tumors

We then investigated whether loss of Prlr in the epithelium changed the histological appearance of SV40T-induced tumors. Tumor tissues were collected and hematoxylin and eosin (H&E) histology was undertaken in a similar manner to C3(1)/SV40T mice described above. There was similar diversity in the microscopic features of lesions observed in tumors taken from mammary gland transplants, the histopathology was comparable to that observed in C3(1)/SV40T mice described above. Areas of necrosis were found in 100% of tumors taken from mice that had reached 10% tumor burden. Only 16/25 and 2/14 palpable tumors collected for histological investigation reached the ethical end point from control C3(1)/SV40T epithelium and Prlr$^{-/-}$/C3(1)/SV40T epithelium, respectively. The large latencies observed in the formation of palpable tumors from these transplants resulted in the lengthening of the experiment beyond the normal healthy life span of a Rag1$^{-/-}$ immune-compromised host. Therefore, a large proportion of tumors were collected before reaching the predetermined end point size. There was little variation in tumor architecture or cellular morphology between tumors derived from mammary glands made from Prlr$^{-/-}$/C3(1)/SV40T epithelium and control C3(1)/SV40T epithelium (Table 2). There was no significant difference in percentage areas of papillary and solid or cellular structure. A small increase was detected in the percentage of tumors that displayed acinar/glandular characteristics in tumors from Prlr$^{-/-}$/C3(1)/SV40T epithelium, but we detected no difference in tumor type (acinar/glandular, papillary and solid) as a function of high and low Prlr expression level in tumors from WT/C3(1)/SV40T epithelium ($P = 0.22$, $P = 0.15$ and $P = 0.54$, respectively; data not shown). This suggests that the small increase in acinar/glandular tumors may simply reflect the longer latency in Prlr$^{-/-}$/C3(1)/SV40T transplants rather than an effect of Prlr. Overall, Prlr null epithelium does not appear to change the mechanism determining the morphology of SV40T-induced tumors.

SV40T-induced neoplasia is delayed in Prlr$^{-/-}$ mammary epithelial cells

In order to determine whether the presence of Prlr in mammary epithelium can modulate the development of SV40T-induced neoplasia, we collected mammary glands made from WT/C3(1)/SV40T and Prlr$^{-/-}$/C3(1)/SV40T epithelial transplants at 22 (154 days) (Figure 5a and b, respectively) and 32 weeks (224 days) (Figure 5c and d, respectively). The Rag1$^{-/-}$ C57BL/6J mouse strain used as our transplant host develops very few mammary ductal side branches (Figure 5e), a feature of this mouse strain that is dependent on factors from the stroma and not the epithelial donor (Naylor and Ormandy, 2002). Thus, donor tissue from a mixed FVB/N and 129Ola/Pas strain develops a mammary tree that shows a predominantly primary ductal branching pattern, formed by bifurcation during ductal elongation at pregnancy (Y-shaped junctions), with sparse side branches (T-shaped junctions), when transplanted into C57BL/6J Rag1$^{-/-}$ hosts. Abnormal development in WT/C3(1)/SV40T transplants first appears as an increased number of short side branches at abnormally close spacing (Figure 5a), a feature that is not seen in control transplants without the C3(1)/SV40T construct. In contrast, Prlr$^{-/-}$/C3(1)/SV40T epithelial transplants at the same age exhibit the same developmental abnormality, but at a greatly reduced frequency (Figure 5b).

To quantify neoplastic area, we assessed the area occupied by SV40T-induced lesions in carmine alum stained Prlr$^{-/-}$/C3(1)/SV40T mammary whole mounts. C3(1)/SV40T mammary epithelium lacking Prlr had a significantly smaller area of total lesions at 22 ($7.6 \pm 1.7\%$; Figure 5f) and 32 weeks ($11.7 \pm 2.4\%$; Figure 5g) compared to control C3(1)/SV40T epithelium (18.4 ± 1.2 and $24.1 \pm 2.8\%$, $P < 0.001$ and $P = 0.005$, respectively). We divided the lesions into neoplasia and tumor. Prlr$^{-/-}$/C3(1)/SV40T transplants also had less neoplastic or tumor area at 22 weeks (7.5 ± 1.6 and $0.2 \pm 0.1\%$, respectively) and 32 weeks (7.3 ± 1.1 and $4.4 \pm 1.6\%$, respectively) than control C3(1)/SV40T

Table 2 Tumor morphology and cellular structure in tumors from WT/C3(1)/SV40T and Prlr$^{-/-}$/C3(1)/SV40T transplants

		Tumor morphology (%)			*Cellular structure (%)*	
Epithelium Genotype	n	*Acinar/Glandular*	*Papillary*	*Solid*	*Type A*	*Type B*
All tumors collected						
WT/C3(1)/SV40T	25	21 ± 4	17 ± 6	61 ± 7	60	40
Prlr$^{-/-}$/C3(1)/SV40T	14	35 ± 6	20 ± 6	45 ± 7	57	43
P-value		0.042	0.76	0.10	χ^2 $P = 0.67$	

n; number of tumors. The average percent of tumor area classified as acinar and/or glandular, papillary and solid is given $\pm$ s.e. The percentage of tumors classified as having type A or type B cellular structure is also shown.

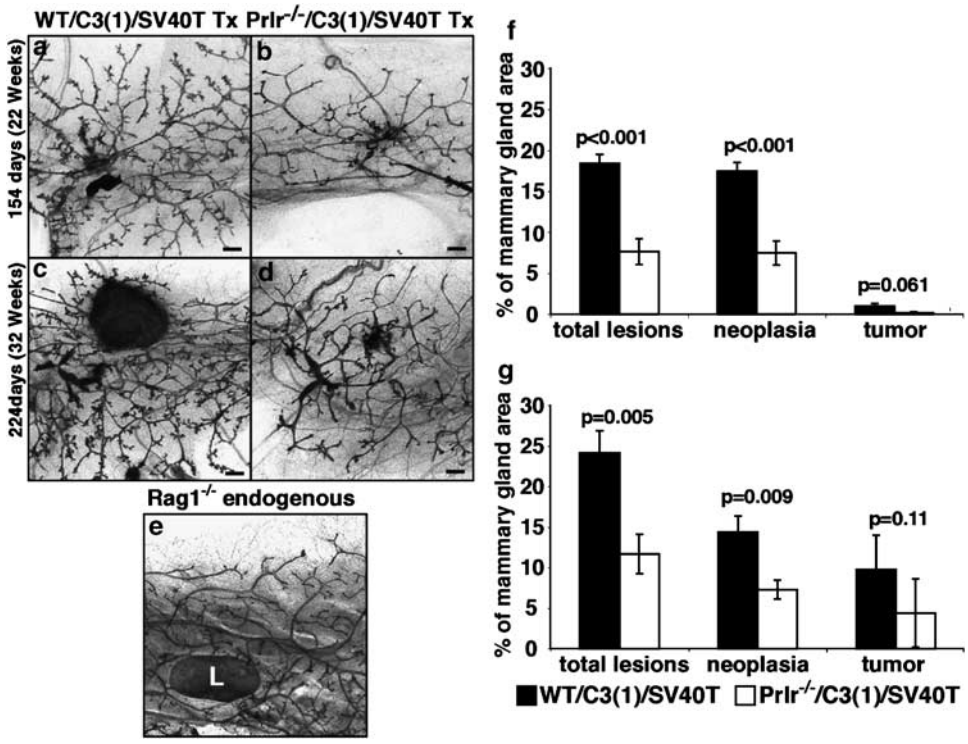

Figure 5 Neoplastic development in Prlr$^{-/-}$/C3(1)/SV40T transplants. Mammary whole mounts of WT/C3(1)/SV40T transplants (**a**, **c**) and Prlr$^{-/-}$/C3(1)/SV40T transplants (**b**, **d**) at 22 weeks (**a**, **b**) and 32 weeks (**c**, **d**) post-transplantation. Scale bars represent 500 μm. Virgin Rag1$^{-/-}$ endogenous inguinal mammary gland whole mount (**e**), L denotes lymph node. Bar graph summary of mammary whole-mount analysis at 22 weeks (**f**) and 32 weeks (**g**). Prlr$^{-/-}$/C3(1)/SV40T transplants (white bars) had less area of total lesions, neoplasia and tumor as a percentage of total mammary gland area compared to WT/C3(1)/SV40T transplants (black bars) at 22 weeks ($P<0.001$, $P<0.001$ and $P=0.061$, respectively) and 32 weeks ($P=0.005$, $P=0.009$ and $P=0.11$, respectively).

transplants at 22 weeks (17.4 ± 1.2 and $1.0\pm0.4\%$; $P<0.001$ and $P=0.06$, respectively) and 32 weeks (14.4 ± 2.0 and $9.8\pm2.6\%$; $P=0.009$ and $P=0.11$, respectively). The ratio of neoplasia to tumor in Prlr$^{-/-}$/C3(1)/SV40T transplants at 22 weeks was greater than in WT/C3(1)/SV40T transplants, however, this ratio equalled control levels by 32 weeks.

Cellular proliferation in SV40T-induced neoplasia is mediated by Prlr within mammary epithelium

H&E histology allows the division of neoplasia into low-grade mammary intraepithelial neoplasia (LGMIN) and high-grade mammary intraepithelial neoplasia (HGMIN). LGMIN displayed the presence of stratified atypical ductal epithelial cells with elongated, hyperchromatic and pleomorphic nuclei. HGMIN were present at multiple foci, and showed greater cellular crowding, more stratification, loss of polarity and increased pleomorphism and hyperchromatism. Often neoplastic cells completely filled the ductal lumen. Invasive lesions are distinguished from HGMIN by breaching the basement membrane and stromal invasion. We used BrdU immunocytochemisty to investigate the effect of Prlr on SV40T-induced cellular proliferation within these lesion types (Figure 6a and b). A significant increase was detected in the proliferation rate of cells from WT/C3(1)/SV40T preinvasive lesions ($17.0\pm1.2\%$) compared to 'typical' WT/C3(1)/SV40T ductal epithelium displaying a normal epithelial morphology ($7.8\pm1.8\%$, Figure 6e; *t*-test $P=0.019$). We detected significantly less proliferation in low-grade and high-grade MIN lesions from Prlr$^{-/-}$/C3(1)/SV40T transplants (11.3 ± 1.2 and $13.0\pm1.4\%$) compared to control C3(1)/SV40T transplants (17.0 ± 1.2 and $17.5\pm2.0\%$ Figure 6e; *t*-test $P=0.003$ and $P=0.067$), demonstrating that loss of Prlr results in reduced SV40T induced proliferation in early stage lesions. There was no significant difference in the number of proliferating cells in invasive lesions from Prlr$^{-/-}$/C3(1)/SV40T transplants compared to control C3(1)/SV40T transplants.

Apoptosis via activation of Caspase-3 is unaltered by Prlr within mammary epithelium

We investigated the effect of a loss of Prlr signaling on apoptosis using an antibody raised against the cleaved and active form of Caspase-3, a marker of cellular apoptosis (Figure 6c and d), We detected no cleaved Caspase-3 positive cells in typical epithelium from both Prlr$^{-/-}$/C3(1)/SV40T and control C3(1)/SV40T transplants. A low level of apoptosis was detected in LGMIN, which increased in HGMIN lesions and was maintained at the same level in invasive lesions. There was no significant difference in the rates of apoptosis in LGMIN, HGMIN and invasive lesions from Prlr$^{-/-}$/C3(1)/SV40T (0.2 ± 0.1, 1.4 ± 0.3 and $1.2\pm0.5\%$) and

control C3(1)/SV40T transplants (0.3 ± 0.1, 1.2 ± 0.2 and $1.3 \pm 0.2\%$, Figure 6F; *t*-tests $P = 0.42$, $P = 0.59$ and $P = 0.92$, respectively). These results indicate that Prlr signaling has no effect on cellular survival via apoptotic mechanisms involving cleavage of Caspase-3 in SV40T-induced lesions.

Discussion

Large-scale prospective studies of breast cancer have demonstrated that prolactin (Hankinson *et al*., 1999; Tworoger *et al*., 2004), estrogen (Missmer *et al*., 2004) and the androgenic precursors of estrogen (Hankinson *et al*., 1998) are hormones that increase the risk of breast cancer in women who experience serum levels within the top quartile of the population range. We have examined how prolactin acts to modulate carcinogenesis, using a model in which mammary cancer is initiated by the SV40T oncogene in the absence or presence of an intact prolactin signaling pathway. Using whole animals or transplanted glands, we have been able to contrast the direct action of prolactin on the mammary epithelial cell with its indirect actions. By a combination of longitudinal survival analysis and cross-sectional histological studies, we have defined the influence of prolactin over latency, numbers and types of tumors produced by SV40T, and we have identified the stage in this carcinogenic process where prolactin acts.

Tumor latency increased as a consequence of the loss of Prlr by 26 days in whole animals (12.0%) and by 53 days (22.5%) in transplants. This comparison shows that the direct effect of prolactin via the mammary epithelial prolactin receptor is the predominant mechanism by which prolactin modulates mammary carcinogenesis. This is also the first demonstration of a mammary cell autonomous effect of prolactin outside of pregnancy. The indirect effects of prolactin are complex. Loss of the prolactin receptor caused reduced estrogen and progesterone levels but increased parathyroid hormone (Clement-Lacroix *et al*., 1999). $Prlr^{-/-}$ mice also had reduced insulin levels and sensitivity (Freemark *et al*., 2001) and decreased body weight. Despite these changes in the endocrine environment, comparison of the difference in relative tumor latency between tumor genotypes in the whole animal (26 days) and transplant experiments (53 days) indicates that the combined effects of these indirect actions on carcinogenesis are negligible.

The stage of the carcinogenic process that is influenced by prolactin has not previously been defined. Transplants lacking Prlr showed greatly reduced areas of neoplasia and longer latency to the first palpable tumor. An analysis of cell proliferation showed a reduction in cell proliferation in the neoplasias as a

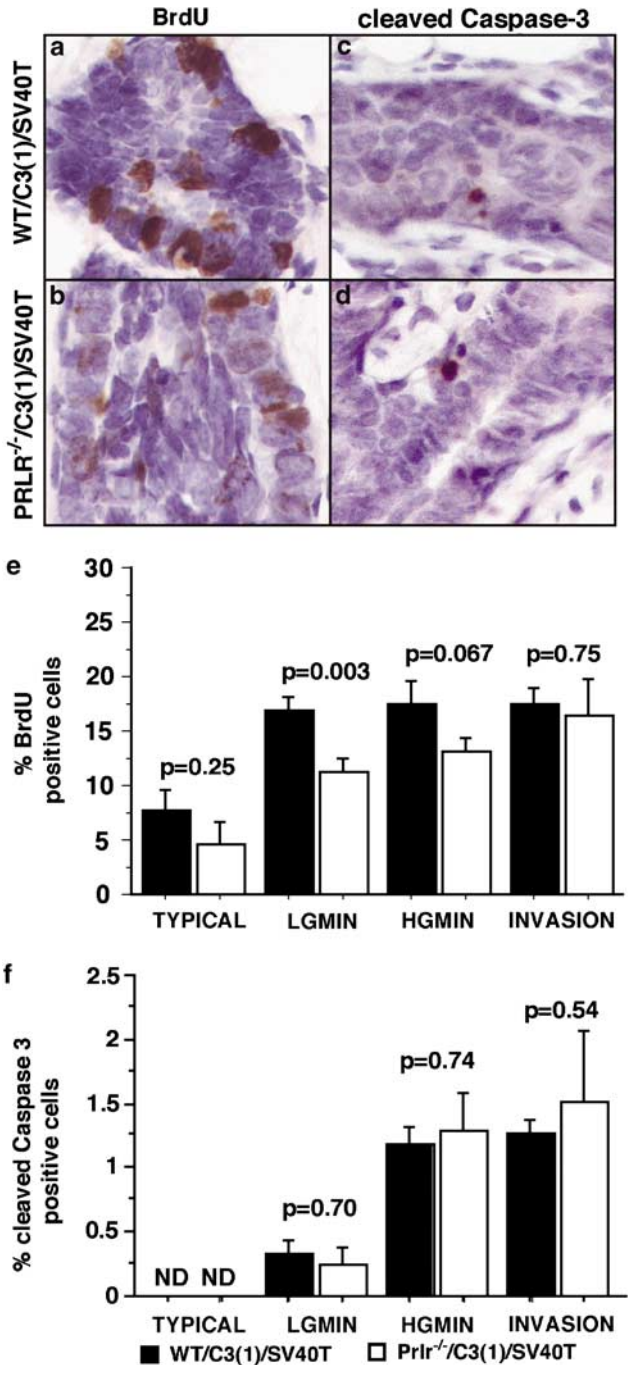

Figure 6 Cellular proliferation and apoptosis in $Prlr^{-/-}$/C3(1)/SV40T epithelium. Immunohistochemistry using antibodies against 5-bromo-2′-dexyuridine (BrdU) in WT/C3(1)/SV40T transplants (**a**) and $Prlr^{-/-}$/C3(1)/SV40T transplants (**b**) and cleaved Caspase-3 in WT/C3(1)/SV40T transplants (**c**) and $Prlr^{-/-}$/C3(1)/SV40T transplants (**d**). (**e**) The percentage of BrdU positive cells in areas of typical ductal epithelium, LGMIN, HGMIN and invasion was reduced in $Prlr^{-/-}$/C3(1)/SV40T transplants (white bars) compared to WT/C3(1)/SV40T transplants (black bars). $Prlr^{-/-}$/C3(1)/SV40T transplants had significantly reduced proliferation via detection of BrdU staining in lesions classified as LGMIN and HGMIN ($P = 0.003$ and $P = 0.067$, respectively). (**f**) There was an undetectable level (ND) of cleaved Caspase-3 staining in typical ductal epithelium from WT/C3(1)/SV40T and $Prlr^{-/-}$/C3(1)/SV40T transplants. There was no significant difference in the rate of apoptosis via measurement of cleaved Caspase-3 in LGMIN, HGMIN and invasive lesions from $Prlr^{-/-}$/C3(1)/SV40T transplants (white bars) compared to WT/C3(1)/SV40T transplants (black bars; $P = 0.42$, $P = 0.59$ and $P = 0.92$, respectively).

result of a loss of the Prlr. Apoptosis was unaffected by genotype at every stage examined. Thus, prolactin acts at the very earliest stages of carcinogenesis to increase cell proliferation in neoplastic lesions, resulting in a greater area of neoplasia and a more rapid emergence of invasive tumors.

We also found that in this model of carcinogenesis, loss of Prlr did not influence the growth of invasive lesions. Overall there was no difference in the proliferation rate or the growth rate of invasive lesions between prolactin genotypes in either the whole animals or the transplants. An analysis of WT tumor transplants showed no relationship between Prlr expression level and tumor growth rate despite the detection of the expected difference between genotypes of latency to palpable tumor. Close inspection of Figure 3b shows a dichotomy of tumor growth rates in $Prlr^{-/-}$ transplants compared to WT. Two distinct types of growth rate are seen in $Prlr^{-/-}$ tumors, a majority with slow growth and three tumors that showed initial slow growth followed by a dramatic increase in growth rate. This dichotomy is reflected in the size of the BrdU error bar for $Prlr^{-/-}$ tumors (Figure 6e). WT tumors show a broad spectrum of growth rates. Although it is tempting to speculate that this difference in growth pattern may reflect a fundamental difference in tumor biology between genotypes, this effect was not seen in whole animals or in relation to Prlr expression level. A few advanced tumors may remain sensitive to prolactin, but in our experiments their frequency was not sufficient to influence the analysis.

Thus, prolactin may facilitate tumor formation in two ways: by increasing the number of neoplastic cells prolactin increases the chance of a tumorigenic event; and by driving the proliferation of neoplastic cells prolactin forces cell divisions that may replicate tumorigenic genetic or epigenetic events. Once these events occur the resulting invasive lesions generally become independent of prolactin. This observation explains why bromocriptine treatment of patients with advanced breast cancer was not successful (Peyrat *et al*., 1984; Bonneterre *et al*., 1988; Manni *et al*., 1989), and why prolactin treatment of breast cancer cell lines does not have a generalized and potent effect on proliferation. Our finding that prolactin acts primarily on neoplastic lesions, and not on subsequent invasive lesions, challenges the prevailing assumption that prolactin acts primarily during late-stage disease to drive invasive tumor growth.

These results have important implications for the treatment of human disease. Agents antagonizing prolactin action, such as S179D prolactin and G129R prolactin (Goffin *et al*., 2005) may prove to be useful in preventing the progression of hyperplastic and neoplastic lesions to invasive cancer. Improvements in imaging and diagnostic techniques are currently under development to allow the identification of these early lesions. Prolactin receptor antagonists should be considered as agents for their treatment, both as an adjuvant to surgery and hormonal therapy, or as a component of preventative therapy.

Materials and methods

Mice and breeding

All experiments involving mice were performed under the supervision and in accordance with the regulations of the Garvan/St Vincent's Animal Experimentation Committee. The $Prlr^{-/-}$ mouse was generated as previously described (Ormandy *et al*., 1997b). The C3(1)/SV40T animals (Maroulakou *et al*., 1994) were on an inbred FVB/N background, and the core colony was maintained by homozygous matings. Mice heterozygous for both $Prlr^{-/-}$ and C3(1)/SV40T were produced by mating homozygous $Prlr^{-/-}$ males and homozygous C3(1)/SV40T females. Female heterozygous progeny were then back crossed to homozygous $Prlr^{-/-}$ males to produce mice heterozygous or wildtype (WT) for C3(1)/SV40T, and $Prlr^{-/-}$. Control WT mice were produced by using WT males in an identical but separate scheme to ensure similar genetic diversity between groups (Robertson *et al*., 2003). $Rag1^{-/-}$ mice (Mombaerts *et al*., 1992) of the C57BL/6J strain were purchased from Animal Resource Centre, Perth, Australia. All animals were housed with food and water *ad libitum* with a 12 h day/night cycle at 22°C and 80% relative humidity. $Rag1^{-/-}$ mice were administered Resprim (Alphapharm, Carole Park, Australia), containing Sulfamethoxazole/Trimethoprim via drinking water (5 mg/1 mg per 5 ml drinking water) in alternate weeks. Mice wild-type for C3(1)/SV40T were weighed weekly and aged to 50 weeks.

Experimental groups

Twenty WT/C3(1)/SV40T and 25 $Prlr^{-/-}$/C3(1)/SV40T mice were observed twice weekly for tumor formation (whole animal study). The date of the first palpable tumor was recorded (age of detection) and tumor size monitored using vernier callipers. The volume of each tumor was estimated using the major and minor axes of palpable tumors (Attia and Weiss, 1966). Mice were killed when the tumor burden reached 10% of the animal's body weight (ethical end point) or earlier if the animal became unhealthy. At killing, tumors were collected for routine H&E histochemistry, and remaining mammary glands were collected for whole mount histology as described below.

Mammary epithelium transplants were performed as previously described (DeOme *et al*., 1959). Approximately 1 cm^3 section of the fourth mammary gland was excised from 5- to 8-week old WT/C3(1)/SV40T and $Prlr^{-/-}$/C3(1)SV40T donors (before the onset of neoplasia) and transplanted into the cleared fourth mammary fat pad of 3-week-old $Rag1^{-/-}$ mice. Two cohorts were generated. The first consisted of 32 $Rag1^{-/-}$ mice with $Prlr^{-/-}$/C3(1)/SV40T donor epithelium and 32 mice with WT/C3(1)/SV40T donor epithelium. This cohort was investigated for the development of palpable tumors as described above. The second cohort comprised 21 mice with $Prlr^{-/-}$/C3(1)/SV40T and WT/C3(1)/SV40T epithelium in alternate inguinal fat pads. Mammary epithelial transplants were collected at 8, 22 and 32 weeks for whole-mount analysis of early neoplastic lesions.

mRNA and protein isolation

Mammary glands from 12-week-old C3(1)/SV40T animals ($n=13$) and 8 ($n=4$), 22 ($n=2$) and 32 week ($n=2$) old mammary glands formed from C3(1)/SV40T epithelium as well as tumors at ethical end point were collected and frozen in liquid nitrogen before storage at −80°C before use. Total RNA was extracted using TRIZOL Reagent (Gibco BRL) according to the manufacturer's instructions.

Whole-mount histology
Mammary whole-mounts were made using the Carmine alum technique as described before (Bradbury *et al*., 1995). Quantitative analysis of neoplasia and tumor was performed using the public domain NIH Image (developed at the US National Institutes of Health and available on the Internet at http://rsb.info.nih.gov/nih-image/). Briefly, the area of neoplasia and tumor (distinguished using whole-mount gross morphology) was estimated by tracing the perimeter of each lesion manually, using photomicrographs of Carmine alum stained whole-mounts imported into NIH Image software. These areas were then converted into a percentage of total mammary gland area. Mammary whole-mounts were then peeled off the slides and paraffin embedded. Sections (4 μm) were cut for routine H&E cytochemistry and immunohistochemistry.

Quantitative PCR
Single-stranded cDNA was produced by reverse transcription using 1 μg RNA in a 20 μl reaction (Promega, WI, USA). Quantitative PCR was performed using LightCycler technology (Roche Diagnostics, Basel, Switzerland). PCR reactions were performed in a 10 μl volume with 1 μl cDNA, 5 pmoles of each primer (SV40T forward CCTGGAATAGTCACCATG, reverse CAATGCCTGTTTCATGCC, Prlr forward GAGA AAAACACCTATGAATGT, reverse GAAGAGCAAGATC TCAAGAAC and Keratin-18 forward TGTTCATAGTGGG CACGGATGTC, reverse CAAGATCATCGAAGACCTGA GGGC (as an epithelial house keeping control). FastStart DNA Master SYBR Green I enzyme mix (Roche) as per manufacturer's instructions. Relative quantitation of the product was performed by comparing the crossing points of different samples normalised to Keratin-18. Each cycle in the linear phase of the reaction corresponds to a two-fold difference in transcript levels between samples. Each reaction was performed in duplicate.

Immunocytochemistry
Mammary gland sections were baked at 80°C for 5 min and placed in xylene for deparaffinisation. Antigen retrieval was performed using target retrieval solution low pH (S1699) 20 min water bath (anti-5-bromo-2′-dexyuridine (BrdU) clone Bu20a) and high pH (S2367) 30 s pressure cooker (anticleaved Caspase-3 Asp175, Cell Signaling Technologies, Beverley MA, USA). Slides were blocked in 3% H_2O_2 and a protein block (anticleaved Caspase-3 only) before application of 1:200 anti-BrdU primary antibody or 1:100 (anticleaved Caspase-3). Secondary antibody was Envision mouse (anti-BrdU) and Envision rabbit (anticleaved Caspase-3) applied for 30 min. Visualization was via diaminobenzidine (DAB +). All immunocytochemistry reagents were purchased from Dako Cytomation (Botany, Australia) unless otherwise stated.

Western blotting
Following RNA extraction using TRIZOL reagent, protein was extracted according to the manufacturer's instructions. Protein (20 μg per lane) was separated using sodium dodecyl sulfate–polyacrylamide gel electrophoresis (SDS-PAGE) (Bio-Rad Laboratories, CA, USA), transferred to polyvinylidine difluoride (Millipore Corp., MA, USA), and blocked overnight with 1% skim milk powder, 50 nM sodium phosphate, 50 mM NaCl, and 0.1% Tween 20. Membranes were incubated with α-SV40T (Santa Cruz, CA, USA) and α-β-actin (Sigma). Specific binding was detected using horseradish peroxidase-conjugated secondary antibodies (Amersham Briosciences, IL, USA) with Chemiluminescence Reagent (PerkinElmer, CT, USA) and Fuji Medical X-ray Film (Fujifilm, Tokyo).

Statistics
The effect of Prlr genotype on the rate of weight gain in whole animals was assessed by the coefficients corresponding to the interactions between genotype and time (β_5, β_6 and β_7) in the following mixed effects model (Laird and Ware, 1982) using the nlme package in R (Pinheiro *et al*., 2005):

$$\begin{aligned}\text{weight}_{ij} = {} & \beta_0 + \text{U}_i + (\beta_1 + \text{V}_i)\text{time}_{ij} + \beta_2\text{genoB}_i \\ & + \beta_3\text{genoC}_i + \beta_4\text{genoD}_i + \beta_5\text{time}_{ij}\text{genoB}_i \\ & + \beta_6\text{time}_{ij}\text{genoC}_i + \beta_7\text{time}_{ij}\text{genoB}_i + \text{error}_{ij}\end{aligned}$$

where i indexes animal and j indexes measurement. y_{ij} is weight measured in grams, genoA (reference), genoB, genoC and genoD represent indicator variables for the four genotypes. Time is measured as weeks since birth and $U_i \sim N(0, \sigma^2_{\text{U}})$ and $V_i \sim N(0, \sigma^2_{\text{V}})$. The effect of genotype on the rate of increase in tumor volume was assessed using a similar model where y_{ij} is the cuberoot of volume, time is days since the detection of a palpable tumor. The difference between Prlr genotypes in terms of mean SV40T mRNA levels, wholemount analyses, BrdU and cleaved Caspase-3 immuno-cytochemistry and tumor morphology was examined by an unpaired t-statistic (Statview, SAS Institute, NC, USA). The difference between Prlr geneotypes in tumor multiplicity was examined by an unpaired t-statistic (Statview). The effect of Prlr genotype on time until detection of a tumor of a defined size, or attainment of ethical end point, was determined by Kaplan Meier survival analysis (logrank statistic) (Statview). The effect of genotype on cellular structure in tumors was determined by a χ^2 statistic (Statview). In all analyses, a $P < 0.05$ corresponded to statistical significance.

Acknowledgements

The Garvan Institute group was supported during the course of this work by The National Health and Medical Research Council of Australia, the Cancer Council New South Wales, The Cooperative Research Center for Innovative Dairy Products and the United States DoD BCRP (DAMD17-03-1-0686 to SRO).

References

Attia MA, Weiss DW. (1966). *Cancer Res* **26**: 1787–1800.
Binart N, Helloco C, Ormandy CJ, Barra J, Clement-Lacroix P, Baran N *et al*. (2000). *Endocrinology* **141**: 2691–2697.
Bonneterre J, Mauriac L, Weber B, Roche H, Fargeot P, Tubiana-Hulin M *et al*. (1988). *Eur J Cancer Clin Oncol* **24**: 1851–1853.
Bonneterre J, Peyrat JP, Beuscart R, Lefebvre J, Demaille A. (1987). *Cancer Res* **47**: 4724–4728.
Bradbury JM, Edwards PA, Niemeyer CC, Dale TC. (1995). *Dev Biol* **170**: 553–563.
Brisken C, Kaur S, Chavarria TE, Binart N, Sutherland RL, Weinberg RA *et al*. (1999). *Dev Biol* **210**: 96–106.

Cardiff RD, Anver MR, Gusterson BA, Hennighausen L, Jensen RA, Merino MJ *et al*. (2000). *Oncogene* **19**: 968–988.
Chen WY, Ramamoorthy P, Chen N, Sticca R, Wagner TE. (1999). *Clin Cancer Res* **5**: 3583–3593.
Clement-Lacroix P, Ormandy C, Lepescheux L, Ammann P, Damotte D, Goffin V *et al*. (1999). *Endocrinology* **140**: 96–105.
Clevenger CV, Chang WP, Ngo W, Pasha TL, Montone KT, Tomaszewski JE. (1995). *Am J Pathol* **146**: 695–705.
Clevenger CV, Furth PA, Hankinson SE, Schuler LA. (2003). *Endocrine Rev* **24**: 1–27.
Das R, Vonderhaar BK. (1997). *J Mammary Gland Biol Neoplasia* **2**: 29–39.
DeOme KB, Faulkin LJJ, Bern HA, Blair PB. (1959). *Cancer Res* **19**: 515–520.
Freemark M, Fleenor D, Driscoll P, Binart N, Kelly P. (2001). *Endocrinology* **142**: 532–537.
Ginsburg E, Vonderhaar BK. (1995). *Cancer Res* **55**: 2591–2595.
Goffin V, Bernichtein S, Touraine P, Kelly PA. (2005). *Endocrine Rev* **26**: 400–422.
Goffin V, Kinet S, Ferrag F, Binart N, Martial JA, Kelly PA. (1996). *J Biol Chem* **271**: 16573–16579.
Green JE, Shibata MA, Yoshidome K, Liu ML, Jorcyk C, Anver MR *et al*. (2000). *Oncogene* **19**: 1020–1027.
Gutzman JH, Miller KK, Schuler LA. (2004). *J Steroid Biochem Mol Biol* **88**: 69–77.
Hankinson SE, Willett WC, Manson JE, Colditz GA, Hunter DJ, Spiegelman D *et al*. (1998). *J Natl Cancer Inst* **90**: 1292–1299.
Hankinson SE, Willett WC, Michaud DS, Manson JE, Colditz GA, Longcope C *et al*. (1999). *J Natl Cancer Inst* **91**: 629–634.
Horseman ND, Zhao W, Montecino-Rodriguez E, Tanaka M, Nakashima K, Engle SJ *et al*. (1997). *EMBO J* **16**: 6926–6935.
Hutchinson JN, Muller WJ. (2000). *Oncogene* **19**: 6130–6137.
Laird NM, Ware JH. (1982). *Biometrics* **38**: 963–974.
Ling C, Hellgren G, Gebre-Medhin M, Dillner K, Wennbo H, Carlsson B *et al*. (2000). *Endocrinology* **141**: 3564–3572.
Llovera M, Pichard C, Bernichtein S, Jeay S, Touraine P, Kelly PA *et al*. (2000). *Oncogene* **19**: 4695–4705.
Manni A, Boucher AE, Demers LM, Harvey HA, Lipton A, Simmonds MA *et al*. (1989). *Breast Cancer Res Treat* **14**: 289–298.
Maroulakou IG, Anver M, Garrett L, Green JE. (1994). *Proc Natl Acad Sci USA* **91**: 11236–11240.
Mershon J, Sall W, Mitchner N, Ben-Jonathan N. (1995). *Endocrinology* **136**: 3619–3623.
Missmer SA, Eliassen AH, Barbieri RL, Hankinson SE. (2004). *J Natl Cancer Inst* **96**: 1856–1865.
Mombaerts P, Iacomini J, Johnson RS, Herrup K, Tonegawa S, Papaioannou VE. (1992). *Cell* **68**: 869–877.
Naylor MJ, Lockefeer JA, Horseman ND, Ormandy CJ. (2003). *Endocrine* **20**: 111–114.
Naylor MJ, Ormandy CJ. (2002). *Dev Dyn* **225**: 100–105.
Ormandy CJ, Binart N, Kelly PA. (1997a). *J Mammary Gland Biol Neoplasia* **2**: 355–364.
Ormandy CJ, Camus A, Barra J, Damotte D, Lucas B, Buteau H *et al*. (1997b). *Genes Dev* **11**: 167–178.
Ormandy CJ, Hall RE, Manning DL, Robertson JF, Blamey RW, Kelly PA *et al*. (1997c). *J Clin Endocrinol Metab* **82**: 3692–3699.
Peyrat JP, Vennin P, Bonneterre J, Hecquet B, Vandewalle B, Kelly PA *et al*. (1984). *Eur J Cancer Clin Oncol* **20**: 1363–1367.
Pinheiro J, Bates D, DebRoy S, Sarkar D. (2005). *R package version* **3**: 1–65.
Reynolds C, Montone KT, Powell CM, Tomaszewski JE, Clevenger CV. (1997). *Endocrinology* **138**: 5555–5560.
Robertson FG, Harris J, Naylor MJ, Oakes SR, Kindblom J, Dillner K *et al*. (2003). *Endocrinology* **144**: 3196–3205.
Rose-Hellekant TA, Arendt LM, Schroeder MD, Gilchrist K, Sandgren EP, Schuler LA. (2003). *Oncogene* **22**: 4664–4674.
Schroeder MD, Brockman JL, Walker AM, Schuler LA. (2003). *Endocrinology* **144**: 5300–5307.
Schroeder MD, Symowicz J, Schuler LA. (2002). *Mol Endocrinol* **16**: 45–57.
Shibata MA, Jorcyk CL, Liu ML, Yoshidome K, Gold LG, Green JE. (1998). *Toxicol Pathol* **26**: 177–182.
Touraine P, Martini JF, Zafrani B, Durand JC, Labaille F, Malet C *et al*. (1998). *J Clin Endocrinol Metab* **83**: 667–674.
Tworoger SS, Eliassen AH, Rosner B, Sluss P, Hankinson SE. (2004). *Cancer Res* **64**: 6814–6819.
Vomachka AJ, Pratt SL, Lockefeer JA, Horseman ND. (2000). *Oncogene* **19**: 1077–1084.
Vonderhaar BK. (1999). *Endocrine-Related Cancer* **6**: 389–404.
Welsch CW, Louks G, Fox D, Brooks C. (1975). *Br J Cancer* **32**: 427–431.
Welsch CW, Nagasawa H. (1977). *Cancer Res* **37**: 951–963.
Wennbo H, Gebre-Medhin M, Gritli-Linde A, Ohlsson C, Isaksson OG, Tornell J. (1997). *J Clin Invest* **100**: 2744–2751.
Wennbo H, Tornell J. (2000). *Oncogene* **19**: 1072–1076.